Microfluidics-based 3D-Printed 4×4 Butler Matrix in Coaxial Technology for Applications up to K Band

V. Palazzi[1], P. Mezzanotte[1], F. Alimenti[1], M. Tentzeris[2], L. Roselli[1]
[1]Department of Engineering, University of Perugia, Perugia, Italy
[2]School of Electrical and Computer Engineering, Georgia Institute of Technology, Atlanta (GA), USA
valentina.palazzi@unipg.it

***Abstract*— This work presents a 4×4 Butler matrix in coaxial technology, realized by combining 3D printing and liquid metal filling. The dielectric part of the coaxial cables is 3D printed using stereolithography. According to such a technology, a liquid photo-reactive resin (i.e., the clear resin V4 from FormLab) is UV cured with a laser beam layer by layer, leading to a solid object. The inner conductor of the coaxial line is implemented with an eutectic Gallium-Indium (GaIn) alloy which is liquid at room temperature and features a conductivity $\sigma = 3.4 \times 10^6$ S/m. The outer conductor, instead, is realized by applying silver nanoparticle ink ($\sigma = 1 \times 10^6$) to the exterior of the 3D-printed circuit and curing the structure at 100°C. Firstly, a branch-line hybrid junction working at 20 GHz has been implemented and measured in order to validate the technology. The magnitudes of the transmission coefficients of direct and coupled ports are equal to about -6 dB, whereas their relative phases are about 90°. Eventually, a complete Butler matrix working at 12 GHz has been optimized with CST and a prototype has been fabricated in order to demonstrate the feasibility of this approach. Transmission coefficients with a magnitude of -12 dB and a phase error of $\pm 6°$ have been obtained at the design frequency, in good agreement with simulations. Although preliminary, these results open the way to a new class of coaxial millimeter-wave circuits and sensors obtained by 3D printing and liquid metal filling methodologies.**

***Keywords*— 3D printing, Butler matrix, coaxial cable, liquid metal, microfluidics, stereolithography**

I. Introduction

Manufacturing technologies for planar circuits are quite mature, enabling the fabrication of high performing circuits up to mm-wave frequencies. Nevertheless, some circuit configurations, characterized by the presence of cross-overs (among them the Butler matrix [1] represents a meaningful example), can run into troubles when realized in 2D surfaces. In some cases, cross-overs are avoided by using 0-dB branch lines [2]. This solution is usually narrow-band and leads to cumbersome circuits. Alternatively, multilayer topologies are adopted [3]. Such an approach, though, leads to more expensive circuits and usually entails the presence of via signals. The latter ones introduce parasitics and uncertainties, which are especially severe moving up with frequencies.

In such a context, 3D manufacturing technologies, enabling the fabrication of objects with arbitrary shapes, have the potential to provide the required degrees of freedom to implement geometrically-complex circuits combining compactness, lightweight and reduced production costs.

Recently, 3D-printing technologies, such as stereolithography and polyjet printing, have been proposed in combination with microfluidics for applications such as sensing [4], reconfigurable antennas [5] or to implement the inner conductor in coaxial cables [6] in the low GHz range (below 6 GHz). The latter application is particularly appealing: indeed, thanks to the adoption of liquid metal, the line impedance of the coaxial cable can be readily varied by changing the diameter of the inner channel of the dielectric scaffolding, thereby extending the applicability of the coaxial technology to RF circuit components with variable line impedance.

This work aims at developing a 4×4 Butler matrix in coaxial technology, realized by combining stereolithography and liquid metal filling. In the following sections a branch line working at 20 GHz is designed, manufactured and validated. After this validation, the design of a first prototype of the matrix scaled to 12 GHz is faced. The design exhibited encouraging performance; eventually, the prototype has been manufactured as a basis for the validation process and preliminary results are reported.

II. Circuit Design and Technology Validation

The schematic of a 4×4 Butler matrix is recalled in Fig. 1. The well-known network consists of four hybrid couplers, two phase-shifters and two cross-overs.

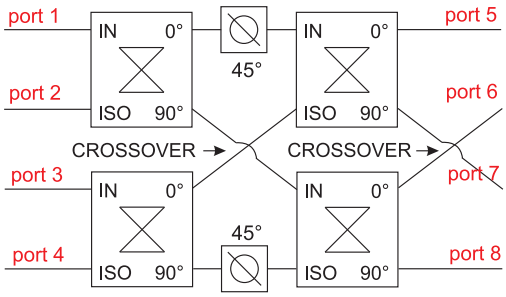

Fig. 1. Schematic of a 4×4 Butler matrix.

In the present work, the whole network is realized in coaxial technology and all ports are matched to 50 Ω. The two cross-overs are implemented by simply arranging transmission lines in a 3D fashion. The phase shifters are implemented with two sections of transmission line as well, while circular branch lines are chosen to implement the hybrids. As a consequence, the network is only made of branch lines and 50 Ω connecting lines. The circuit is designed with the help of CST Microwave Studio.

The next two sections are dedicated to the description of the adopted manufacturing techniques and to the design and validation of the single branch line.

A. *Adopted materials and technology*

The dielectric part of the coaxial cables is 3D printed by using the Form2 printer by FormLabs. This low-cost printer is based on the stereolithography technology. According to this technology, a liquid photo-reactive resin is UV cured with a laser beam layer by layer, leading to a solid object. The adopted resin is the clear material V4 [7] and the maximum allowed resolution, corresponding to a layer thickness of $25\,\mu$m, is chosen to guarantee the highest level of detail.

The adopted material is firstly electromagnetically characterized in waveguide, according to the Nicholson-Ross-Weir method [8]. Bricks of material are manufactured and tested. From the experimental results, a permittivity ϵ_r of 2.7 is obtained at 12 GHz, while $\epsilon_r = 2.65$ is found at 20 GHz. The loss tangent is equal to 0.03 at both frequencies.

Unlike in [6], where a coaxial cable is manufactured by using polyjet printing and the volume destined for the inner conductor is also 3D printed with a dissolvable wax-like support material, the Form2 printer can print one material at a time, so the channels corresponding to the inner conductor have been left empty. The adopted technology is not optimized to perform accurate microfluidics channels, but it is extremely low cost if compared to the former one. Therefore, in the present work the limits of the Form2 printer are challenged to achieve the best possible control of the channel formation.

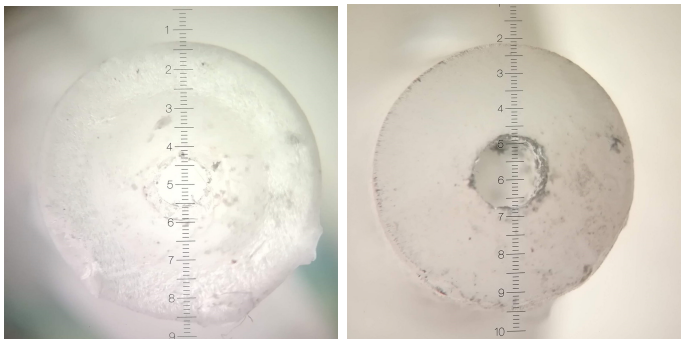

(a) (b)

Fig. 2. Photos at microscope of a fabricated channels. In (a) the diameter of the channel is set to 0.95 mm, while the measured one is 0.656 mm. In (b) the diameter of the channel is set to 1.3 mm, while its measured value is 1.029 mm. Each scale division corresponds to $57.2\,\mu$m.

First of all, channels with different radii have been fabricated. It has been observed that a systematic error is introduced in the manufactured prototypes corresponding to a reduction of $150\,\mu$m in the radius. Fig. 2 shows two photos of the cross-section of manufactured channels. Therefore, this offset is pre-compensated in the circuit model. The circuit orientation during the printing process is also of paramount importance to avoid that excess material is trapped in the channels and finally cured with the prototype, leading to channel restriction or even blockage. In particular, it has been observed that the circuit must be oriented so that the interior channels are placed as vertically as possible with respect to the plate of the printer. Additionally, isopropyl alcohol is pumped into the channels of the prototype before curing to remove any residual material.

To implement the inner conductor, the eutectic gallium indium (GaIn) alloy from Sigma Aldrich is adopted. This metal alloy is liquid at room temperature and features a good conductivity ($\sigma = 3.4\times10^6$ S/m)). The liquid metal is directly pumped in the channels with a syringe.

On the other hand, the outer conductor of the coaxial cable is realized by applying $3/4$ layers of silver nanoparticle ink ($\sigma = 1\times10^6$) to the exterior of the 3D printed circuit. After each ink deposition, the circuit is cured at 100° for 30 minutes. The connectors are attached to the prototypes only after metalization to avoid that the GaIn, which expands when exposed to high temperature, would damage the circuit. Finally, a colloidal silver paste is used to assure the electrical connection between the outer conductor of the 3D printed coaxial cable and the outer conductor of the SMAs. The conductivity of the paste is similar to the one of silver nanoparticle ink ($\sim 10^6$ S/m).

B. *Coaxial branch line*

To test the performance of the proposed manufacturing process a single branch line operating at 20 GHz is designed and manufactured. Fig. 3 shows the main dimensions of the circuit and some of the manufacturing steps of the prototype.

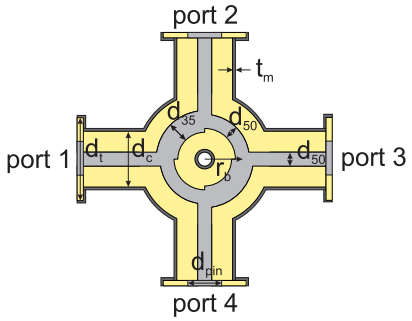

(a)

(b) (c)

Fig. 3. Branch line: (a) cross-section view of the layout, (b) photo of the manufactured dielectric scaffolding and (c) photo of the inner conductor. The main circuit parameters are: $d_c = 2.5$ mm, $d_t = 4$ mm, $d_{50} = 0.6$ mm, $d_{35} = 0.93$ mm, $d_{pin} = 1.25$ mm, $r_b = 1.65$ mm, $t_m = 5\,\mu$m.

Due to the reduced diameter of the branch line at 20 GHz, the diameter of the coaxial cable is set to 2.5 mm, which leads to a channel diameter of just 0.6 mm for a $50\,\Omega$ line.

A step transition is then added at the end of the four lines corresponding to the ports of the branch to adapt the circuit to the SMA connector diameter.

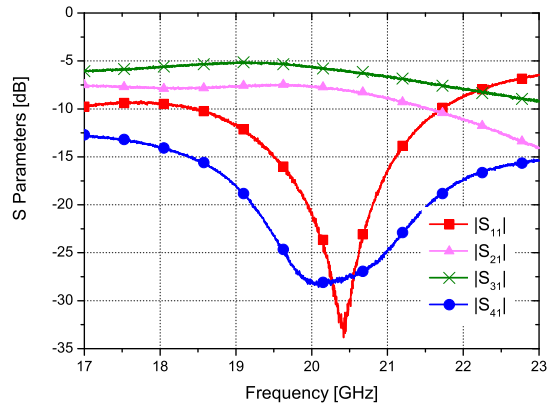

(a)

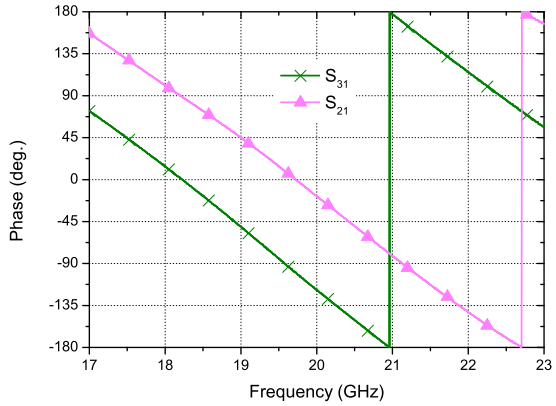

(b)

Fig. 4. Measured scattering parameters of the proposed coaxial branch line at 20 GHz. (a) magnitude and (b) phase.

The S-parameters of the branch line are measured with a vector network analyzer and the results are shown in Fig. 4.

The circuit is centered at the design frequency of 20 GHz, with a slight frequency up-shift of the minimum input reflection coefficient and a slight frequency down-shift of the maximum coupling. The measured maximum transmission coefficients (magnitudes) of direct and coupled ports are about -5.5 and -7.2 dB, respectively. These results accounts for both dielectric and conductor losses of the designed coaxial structure, including those of the feeding lines, and the manufacturing tolerances. The circuit features a minimum input reflection coefficient of -33 dB ($|S_{11}| < -10$ dB from 18.5 to 21.8 GHz) and maximum isolation of 28 dB. The transmission coefficients of the direct and coupled ports are 90° out of phase at the design frequency.

III. Butler Matrix Results

The complete Butler matrix is then designed and manufactured. The circuit is scaled to 12 GHz to relax the requirement on the interior channel diameter ($d_{50} = 1$ mm, $d_{35} = 1.55$ mm, $d_c = 4$ mm, $r_b = 2.7$ mm).

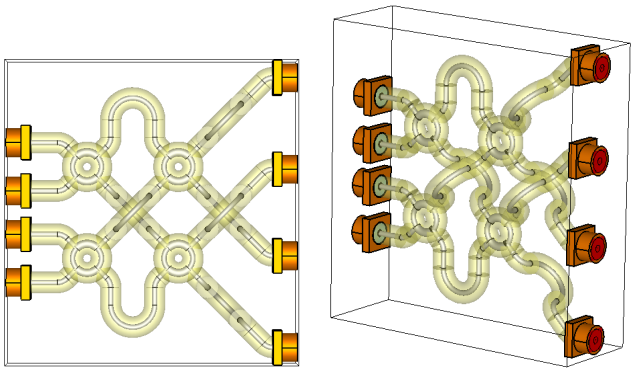

(a) (b)

Fig. 5. Layout of the proposed Butler matrix: (a) front and (b) perspective views. Total volume occupation: $45.4 \times 51.5 \times 15\text{mm}^3$.

Fig. 5 shows the developed CAD model where the outer conductor is removed and the dielectric material is made transparent to show the interior of the circuit. Curved lines are used to implement the two cross-overs. Identical curved lines are also used for the other two output lines (connected to ports 5 and 8) to guarantee that all the four output lines feature the same electrical length.

This circuit is manufactured with the afore described process and the obtained prototype is shown in Fig. 6. Fig. 6(a) illustrates the 3D printed dielectric scaffolding in the optimal orientation to avoid channel blockage. The scaffolding alone weighs 5 grams, while the complete circuit including the eight connectors weighs 17 grams.

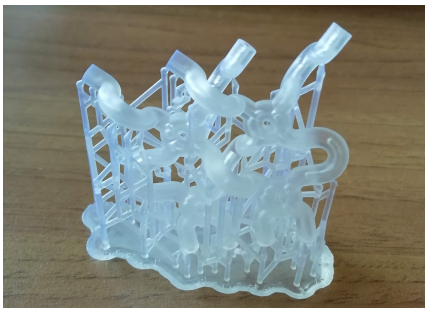

(a)

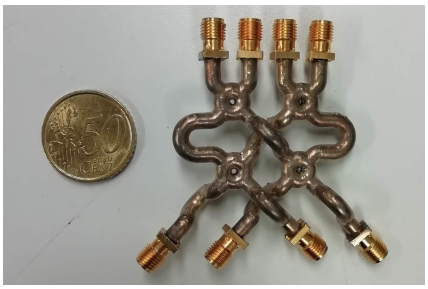

(b)

Fig. 6. Prototype of the proposed coaxial Butler matrix: (a) dielectric scaffolding still attached to the support material and (b) final prototype.

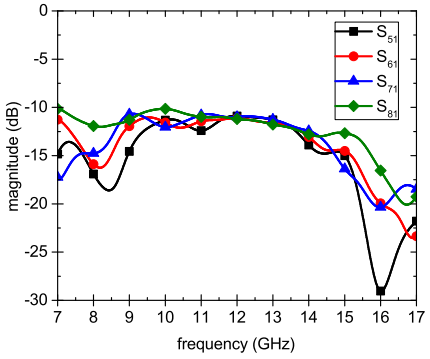

(a)

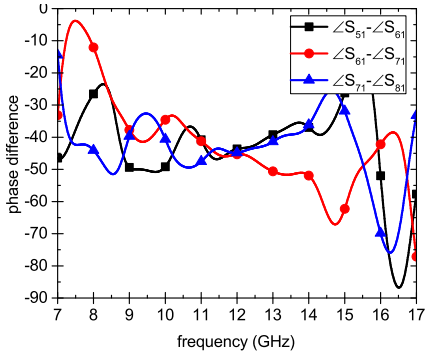

(b)

Fig. 7. Simulated S-parameters of the Butler matrix. (a) Magnitude and (b) phase difference of the transmission coefficients of the Butler matrix entering from port 1.

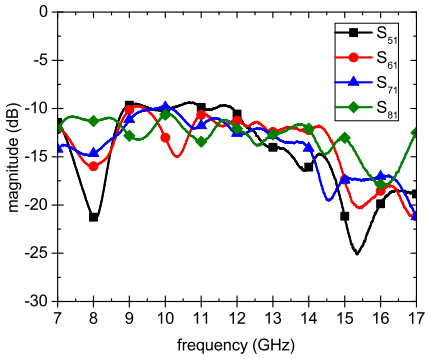

(a)

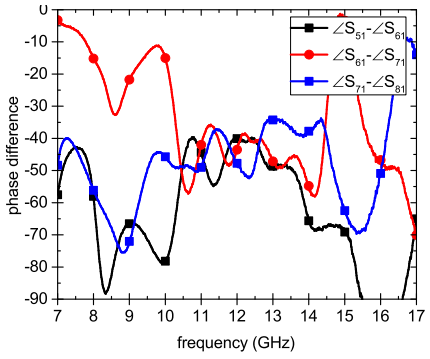

(b)

Fig. 8. Measured S-parameters of the Butler matrix. (a) Magnitude and (b) phase difference of the transmission coefficients of the Butler matrix entering from port 1.

Simulated results (i.e., transmission coefficients entering from port 1) are reported in Fig. 7. The matrix is centered at the design frequency. About 5 dB of losses are observed due to the dielectric and conductor loss. An accuracy among the phase differences of the transmission coefficients of about 4° is obtained at the design frequency.

The transmission coefficients of the matrix are measured as well. As illustrated in Fig. 8, a satisfactory agreement with the simulations is obtained in the range $11 - 13$ GHz. The slightly higher losses (around $1 - 2$ dB) that are experienced in the measurement results are due to surface roughness and fabrication tolerances, which are not taken into account in the simulations. The phase error at the design frequency is $\pm 6^\circ$.

IV. Conclusion

A 3D printed Butler matrix in coaxial technology has been fabricated for the first time by using a low-cost stereolithography technology and a liquid metal. The manufacturing process has been optimized to guarantee a controllable channel cross-section and reduce prototyping failures. A single branch line has been manufactured and tested, showing a very promising performance at the operating frequency of 20 GHz. A scaled version of the complete matrix has also been designed and manufactured. The simulated values obtained by introducing the actual electromagnetic parameters of the adopted materials compare well with the obtained experimental results. There is also margin for improvement by optimizing the assembling procedure. This work opens the way to a new class of coaxial millimeter-wave circuits and sensors obtained by 3D printing and liquid metal filling methodologies.

References

[1] J. Butler, "Beam-forming matrix simplifies design of electronically scanned antennas," *Electronic design*, vol. 12, pp. 170–173, 1961.

[2] V. Palazzi, P. Mezzanotte, and L. Roselli, "A Novel Agile Phase-Controlled Beamforming Network Intended for 360 Angular Scanning in MIMO Applications," in *2018 IEEE/MTT-S International Microwave Symposium - IMS*, Jun. 2018.

[3] C.-C. Chang, R.-H. Lee, and T.-Y. Shih, "Design of a beam switching/steering butler matrix for phased array system," *IEEE Trans. Antennas Propag.*, vol. 58, no. 2, pp. 367–374, 2010.

[4] S. Moscato, M. Pasian, M. Bozzi, L. Perregrini, R. Bahr, T. Le, and M. M. Tentzeris, "Exploiting 3D printed substrate for microfluidic SIW sensor," in *2015 European Microwave Conference (EuMC)*, Sep. 2015.

[5] W. Su, S. A. Nauroze, B. Ryan, and M. M. Tentzeris, "Novel 3D printed liquid-metal-alloy microfluidics-based zigzag and helical antennas for origami reconfigurable antenna "trees"," in *2017 IEEE MTT-S International Microwave Symposium (IMS)*, Jun. 2017.

[6] J. Shen, D. P. Parekh, M. D. Dickey, and D. S. Ricketts, "3D Printed Coaxial Transmission Line Using Low Loss Dielectric and Liquid Metal Conductor," in *2018 IEEE/MTT-S International Microwave Symposium - IMS*, Jun. 2018.

[7] "Clear Resin 1 L RS-F2-GPCL-04." [Online]. Available: https://formlabs.com/it/store/eu/form-2/materials/clear-resin/

[8] W. B. Weir, "Automatic measurement of complex dielectric constant and permeability at microwave frequencies," *Proc. IEEE*, vol. 62, no. 1, pp. 33–36, 1974.